Journal of Peptide Science
J. Peptide Sci. **4**: 413–425 (1998)

Microscopic Observations of the Different Morphological Changes Caused by Anti-bacterial Peptides on *Klebsiella Pneumoniae* and HL-60 Leukemia Cells

SIU CHIU CHAN, WAN LUNG YAU[1], WEI WANG, DAVID KEITH SMITH, FWU-SHAN SHEU and HUEIH MIN CHEN*

Department of Biochemistry, Hong Kong University of Science and Technology, Clear Water Bay, Kowloon, Hong Kong

Received 22 December 1997
Accepted 7 March 1998

Abstract: Natural anti-bacterial peptides cecropin B (CB) and its analogs cecropin B-1 (CB-1), cecropin B-2 (CB-2) and cecropin B-3 (CB-3) were prepared. The different characteristics of these peptides, with amphipathic/hydrophobic α-helices for CB, amphipathic/amphipathic α-helices for CB-1/CB-2, and hydrophobic/hydrophobic α-helices for CB-3, were used to study the morphological changes in the bacterial cell, *Klebsiella pneumoniae* and the leukemia cancer cell, HL-60, by scanning and transmission electron microscopies. The natural and analog peptides have comparable secondary structures as shown by circular dichroism measurements. This indicates that the potency of the peptides on cell membranes is dependent of the helical characteristics rather than the helical strength. The microscopic results show that the morphological changes of the cells treated with CB are distinguishably different from those treated with CB-1/CB-2, which are designed to have enhanced anti-cancer properties by having an extra amphipathic α-helix. The morphological differences may be due to their different modes of action on the cell membranes resulting in the different potencies with lower lethal concentration and higher concentration of 50% inhibition (IC_{50}) of CB on bacterium and cancer cell, respectively, as compared with CB-1/CB-2 (Chen *et al.* 1997. *Biochim. Biophys. Acta 1336*, 171–179). In contrast, CB-3 has little effect on either the bacterium or the cancer cell. These results provide microscopic evidence that different killing pathways are involved with the peptides. © 1998 European Peptide Society and John Wiley & Sons, Ltd.

Keywords: modes of action; anti-bacterial; cecropins; morphology.

INTRODUCTION

Cecropins were originally discovered in the pupae of the cecropia moth (*Hyalophora cecropia*) [1] and are involved in humoral immune responses against intruders such as non-pathogenic bacteria [2]. More recently, other non-mammalian and mammalian cecropins were isolated from the fly, *Drosophila* [3], and from pig intestine [4]. High concentrations of peptides including cecropins A, B, D and P1 were purified from these two insects and pigs by traditional chromatographic methods [5,6]. These pep-

Abbreviations: CB, cecropin B; CB-1, cecropin B-1; CB-2, cecropin B-2; CB-3, cecropin B-3; CD, circular dichroism; D.PBS, Dulbecco's phosphate-buffered saline; FBS, fetal bovine serum; HL-60, HL-60 leukemia cell; HFP, 1,1,1,3,3,3-hexafluoro-2-propanol; KP, *Klebsiella pneumoniae*; LC, lethal concentration; MASV, major axis section view; MISV, minor axis section view; SEM, scanning electron microscopy; TEM, transmission electron microscopy.

* Correspondence to: Department of Biochemistry, Hong Kong University of Science and Technology, Clear Water Bay, Kowloon, Hong Kong.

[1] Current address: Department of Histopathology, Queen Mary Hospital, Hong Kong.

CCC 1075–2617/98/070413-13$17.50

tides have the specific function of killing microbes and are classified as anti-bacterial peptides. The natural peptides have limited ability to kill microbes and therefore to improve the killing ability, non-natural peptides need to be produced. Solid-phase chemical synthesis [7] and biological synthesis using recombinant DNA techniques [8,9] can be utilized to produce these peptides. Of these two methods, the former has been well developed and widely used. As the resistance of bacteria to chemical anti-microbial agents [10] increases, peptide antibiotics [11] such as cecropin [1], melittin [12,13], magainin [14], and defensin [15], will have an influential role and may be widely used in the future.

In addition to the cecropins' anti-bacterial function, their inability to lyse healthy mammalian cells [14] while being capable of attacking transformed cells [16,17] may make them potentially useful as peptide anti-cancer drugs (a different strategy to the currently used chemical anti-cancer agents [18]). Our previous report [17] has shown that certain custom cecropin-like peptides (e.g. CB-1 and CB-2) have a greater ability to lyse cancer cells but are less effective on bacteria when compared with naturally produced CB. In this paper, we focus mainly on the area of morphological changes induced by cecropin B and its analogs, CB-1, CB-2 and CB-3 on the bacterium, *Klebsiella pneumoniae* (KP), and the cancer cell, HL-60 leukemia (HL-60). The different morphological changes of the cells induced by the different characteristics of the peptides may possibly be related to the different potencies of these peptides on cell membranes [17].

MATERIALS AND METHODS

Materials

The strains of KP and HL-60 used were obtained from the American Type Culture Collection (ATCC), USA. Penicillin and streptomycin were products of Gibco (USA). Absolute ethanol, glutaraldehyde, and sodium cacodylate were obtained from Merk (USA), Sigma (USA) and BDH (UK), respectively. Propylene oxide and osmium tetroxide were obtained from Sigma. The cell culture medium, RMPI-1640, was the product of Sigma. The fetal bovine serum (FBS) and Dulbecco's phosphate-buffered saline (D.PBS) were purchased from Gibco. The 1,1,1,3,3,3-hexafluoro-2-propanol (HFP) was the product of Sigma. The water used in this experiment was deionized and distilled.

Peptide Synthesis

The peptides were synthesized using the solid-phase method originally described by Merrifield [7]. CB, CB-1, and CB-2 were generated by an Applied Biosystems (ABI) 431 Peptide Synthesizer and were described previously [17]. Cecropin B-3 (CB-3) was prepared by replacing the N-terminal 1–10 segment of CB with the C-terminal sequence of CB (positions 25–35). After purification using reversed phase HPLC, the purity, molecular weight, peptide content and amino acid composition of CB, CB-1, and CB-2 were as determined previously [17]. For CB-3, a new analog peptide used in this experiment, was prepared by the same peptide synthesizer. Fmoc chemistry was applied with HBTU/HOBT coupling. The final product was deprotected and cleaved from the resin and the resin itself was removed by filtration. CB-3 peptide was precipitated with diethyl ether after the organic solvents were evaporated. The crude materials were desalted on Sephadex G-10 and purified using reverse phase HPLC (Vydac C-18 column) (see Figure 1a for CB-3's purity). The desired product has been estimated to be sufficiently pure for microscopic investigations. The molecular weight of the peptide was determined by mass spectroscopy (Finnigan MAT VISION 2000) with the theoretical and found values of 3556.34 and 3555.36, respectively. The peptide content was calculated by performing quantitative amino acid analysis (AAA) with norleucine as an internal reference amino acid. Results of the amino acid compositions and the amino acid ratios for CB-3 are shown in Table 1. The sequences of these peptides are shown in Figure 1b. The concentrations of the peptide stock solutions were determined by the net weights of the peptides and their molecular weights.

Circular Dichroism (CD) of Peptides

A spectropolarimeter (Jasco Model J-720) was used to investigate the secondary structure of the peptides, CB, CB-1, CB-2 and CB-3. The concentrations of CB, CB-1, CB-2 and CB-3 used for CD measurements were 0.07 mg/ml and the solution pH was adjusted to 6.4 in 2.5 mM sodium phosphate buffer. Detailed descriptions of the CD measurements were given in [17].

Scanning Electron Microscopy (SEM) on KP

KP was inoculated into a Luria-Bertani (LB) medium and grown in a shaker at 37°C overnight. The bacterial culture was centrifuged in a 15 ml

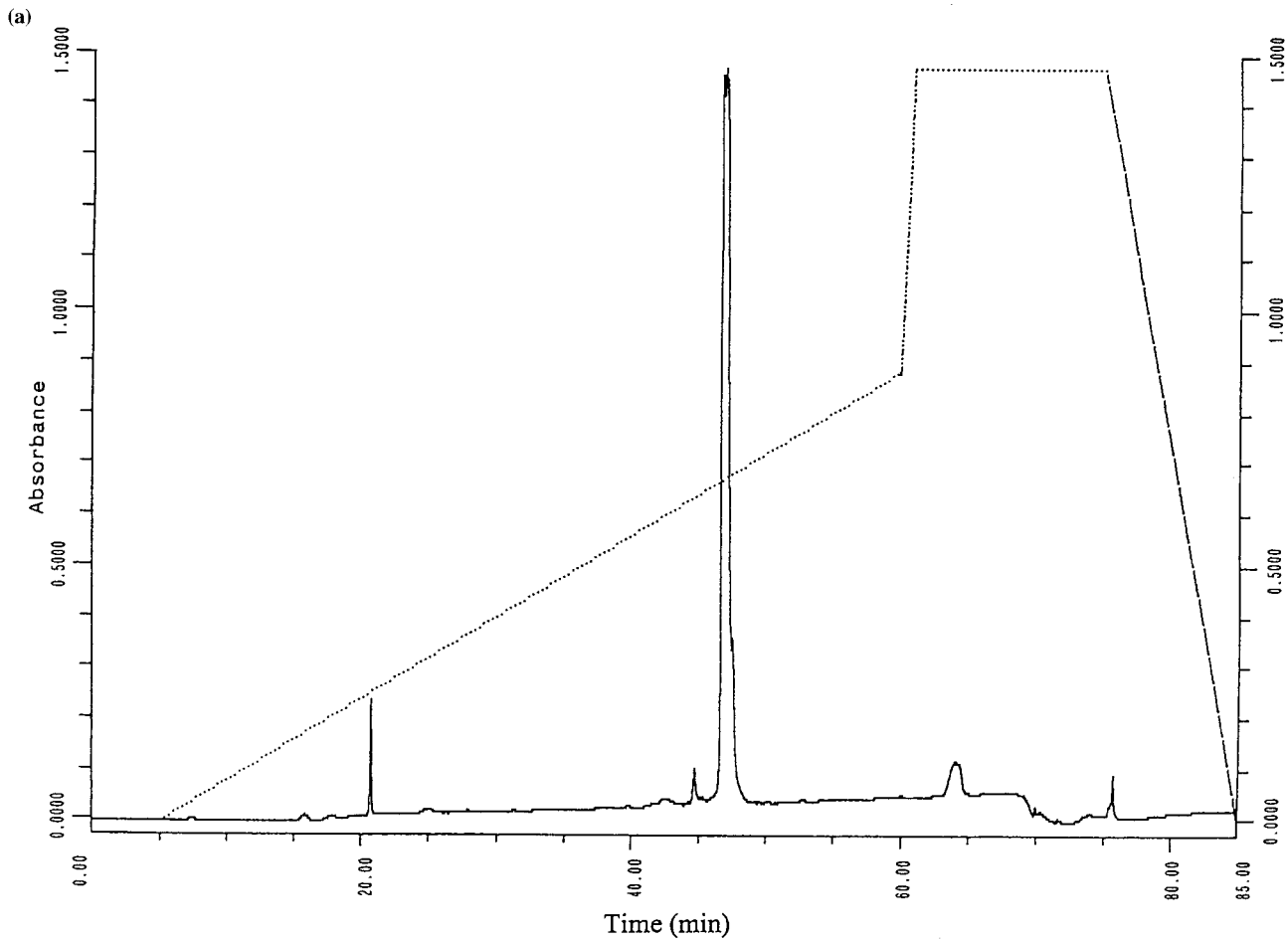

Figure 1 (a) Analytical reversed phase HPLC of the synthetic CB-3. The elution was done by using buffer A (100% H_2O, 0.1% TFA) and buffer B (100% CH_3CN, 0.1% TFA) with the linear gradient of buffer B from 0 to 60% shown by the dotted line. The plateau indicates 100% of buffer B was reached. The flow rate was set at ml/min. The CB-3 peptide was eluted after 47 min. (b) Amino acid sequences of natural cecropin B (CB) and custom-designed cecropins CB-1, CB-2 and CB-3. In CB, the first underlined segment is a probable amphipathic helix (the NMR structure of CB is currently being investigated in this laboratory) and the second underlined segment is a probable hydrophobic helix. CB-1 was constructed by repeating the segment from positions 1 to 10 of CB (underlined in CB) in the region between position 25 and the C-terminus of CB-1 (underlined in CB-1). CB-2 is similar to CB-1 but with the addition of a Gly-Pro residue pair immediately after Pro-24. CB-3 was constructed by repeating the segment from positions 25 to 35 of CB (underlined in CB) in the region between positions 1 and 11 of CB-3 (underlined in CB-3).

tube at 5000 rpm for 10 min at 4°C and then washed two times with 150 mM NaCl. After this, the KP pellet was resuspended in 150 mM NaCl and then diluted to an $OD_{550\ nm}$ of 0.5. The diluted solution (450 μl) was mixed with a freshly prepared cecropin solution (50 μl at 500 μM). A control sample was prepared by adding D.PBS buffer instead of the peptide solution. Samples were placed in 1.5 ml Eppendorf tubes and smoothly rotated at room temperature for 2 h. After this, the Eppendorf tubes

Table 1 Amino Acid Analysis of CB-3 Peptide

Amino acid	P moles	Mole %	AA ratio	AA comp.	
				Experimental	Theoretical
Asp	1356.6	5.427	1.949	1.960	2.000
Glu	1472.9	5.892	2.117	2.128	2.000
Pro	759.4	3.038	1.091	1.097	1.000
Gly	3399.4	13.599	4.885	4.912	5.000
Ala	6481.3	25.927	9.314	9.366	9.000
Val	1707.4	6.830	2.454	2.467	3.000
Met	695.9	2.784	1.000	1.006	1.000
Ile	2441.0	9.765	3.508	3.527	4.000
Leu	3013.2	12.054	4.330	4.354	4.000
Lys	2339.1	9.357	3.361	3.380	3.000
Arg	1331.8	5.328	1.914	1.925	2.000

The total AA (experimental) = 36.124. The total AA (theoretical) = 36.000.

were centrifuged at 5000 rpm for 5 min and the supernatant was removed. The pellet was resuspended in 500 μl of 2.5% glutaraldehyde in 0.1 M of sodium cacodylate buffer. The fixed samples (200 μl) were further filtered using a polycarbonate membrane filter with a pore size of 0.22 μm. Dehydration of the sample was then conducted by a series of soakings in two-repeated washing steps using 30, 50, 70, 90 and 100% ethanol. The specimens were further dried by using a critical-point dryer (Pelco, CPD2). These samples were mounted on aluminium stubs covered by an adhesive epoxy tape and were then coated with gold to a thickness of 200 nm by using a sputter coater (Demon). The treated KP cells were then examined using a Leica 440 SEM microscope.

Transmission Electron Microscopy (TEM) on KP

Preparation of KP for the TEM study was similar to that for the SEM investigations. After preparation, peptide solutions (50 μl at 500 μM) were added to the washed KP suspension (450 μl at $OD_{550\ nm}$ = 1.0). The mixture was incubated for 2 h and then spun down. The pellet was briefly fixed with 500 μl of 2.5% glutaraldehyde in 0.1 M sodium cacodylate–HCl buffer at pH 7.4. The tissue blocks were then extracted and cut into sizes of 1 mm^3. These pieces were fixed in 2.5% glutaraldehyde in a cacodylate buffer (0.1 M sodium cacodylate–HCl buffer at pH 7.4) for 2 h. After fixation, the solution was replaced by cacodylate buffer with 0.1 M sucrose and the tissue blocks were washed several times with cacodylate buffer to remove excess fixatives. Post-fixation was conducted by putting the sample in 1% osmium tetroxide in cacodylate buffer for 1 h at room temperature. Dehydration of the sample was then carried out on a rotary shaker after the tissue blocks had been further washed by several changes of cacodylate buffer. The samples were dehydrated by successive soakings in 50, 70 and 90% ethanol for 5 min each, three soakings in 100% ethanol for 10 min each and two soakings in propylene oxide for 5 min each. The dried tissues were then infiltrated by a mixture of epoxy resin and propylene oxide (1:1 v/v) for 1.5 h at 37°C, then by a mixture of epoxy resin and propylene oxide (3:1 v/v) overnight at room temperature, and finally by epoxy resin alone for 1 h at 37°C. After infiltration, plastic capsules (Micron Moulds) were used to embed the tissue blocks, which were then polymerized at 60°C overnight. These samples were removed from the plastic capsules using blades and were trimmed to a trapezoid shape. Ultrathin sections (90 nm) were made by using an ultramicrotome and mounted on 200 mesh copper grids. Following this, the sections were stained by 2% aqueous uranyl acetate for 20 min, washed well by distilled water, stained by Reynold's lead citrate for 15 min, and washed again with distilled water. Air-drying was applied and the sections were stored in a labeled Petri disc. TEM images of the specimens were then obtained using a JEOL 100SX transmission electron microscope at 100 kV.

SEM on HL-60

HL-60 cells were maintained in a RMPI-1640 medium supplemented with 10% FBS. The seeding density was about 1×10^5 cells/ml. The cells were

harvested after culturing for 2 days and were washed two times with D.PBS and resuspended in RMPI-1640 with 0.5% FBS. The HL-60 cells in a RMPI-1640 medium (450 μl) with 0.5% FBS at a concentration of 1×10^6 cells/ml were seeded in a 24-well plate. The plate was incubated at 37°C, 95% air/5% CO_2 overnight. A 50 μl volume of D.PBS buffer and peptide solutions (500 μM) were added to the control and test wells, respectively. The plate was then maintained in the incubator with 95% air/5% CO_2 at 37°C for 15 min. Subsequently, 500 μl of 5% glutaraldehyde in 0.1 M sodium cacodylate buffer were added into the wells. The solutions were left for 2 h at 4°C and then 50 μl of the fixed sample were drawn into a syringe. The sample was filtered through a 0.45 μm polycarbonate membrane filter (Millipore) held in a Swinnex membrane filter adapter (Millipore). The remaining steps for SEM sample preparation were as described in the section describing SEM on KP cells. The SEM images of the HL-60 cells were then examined by a JEOL 6300F SEM microscope with a cold-cathode field emission electron gun.

TEM on HL-60

Preparation of HL-60 cells for the TEM study was as described for the SEM investigation. After adding peptide solution and fixation, 800 μl of the test cells in 2.5% glutaraldehyde in a 1.5 ml Eppendorf tube were centrifuged at 1000 rpm for 5 min. The pellet was resuspended by adding a small amount of 8% bovine serum albumin (BSA) in 0.05 M Tris buffer at pH 7.3. The solution was immediately centrifuged at 1500 rpm for 5 min. Small amounts of 25% glutaraldehyde were slid into the mixture and centrifuged immediately at 2500 rpm for 5 min. The remaining procedures such as gelling, fixation, dehydration, polymerization and finally the generation of ultrathin sections were similar to the procedures used for KP cells (see section 'TEM on KP'). TEM images of the specimens were then obtained using a JEOL 100SX transmission electron microscope at 80 kV.

Toxicity Measurements

The lethal concentration (LC) measurements and the cytotoxicity assays (IC_{50}) have been described elsewhere in detail [17]. In this experiment, the LC (mol/l) was determined from the slope of the plot of η^2 versus ϖ due to the following equation:

$$\eta^2 = (0.47/\lambda\ \mathrm{LC})\varpi \qquad (1)$$

where η indicates the zone diameter with unit of dm, ϖ represents moles of peptide and λ is the thickness of the agarose in the plate (0.025 dm in this experiment). The IC_{50} was determined from the curve of cell survival versus concentration of peptide and taken from the concentration at which cell viability was 50%. The cell survival was measured by using microtetrazolium (MTT)-based colorimetric assay.

RESULTS

CD and the Potency Measurements of CB, CB-1, CB-2 and CB-3

Figure 2 shows the CD curves of CB, CB-1, CB-2 and CB-3 without HFP (group I) and with 20% (v/v) of HFP (group II). In group I, when HFP was not in the solution, a negligible CD effect (random coil) for all peptides was observed. In group II, the constituents of the secondary structures were analysed and this showed that the α-helical contents of peptides were approximately equal (CB: 56.6%; CB-1: 52.4%; CB-2: 50.4%; CB-3: 53.3%).

The LC values of CB, CB-1 and CB-2 were 0.26, 0.39, and 0.36 μM, respectively, and the IC_{50} values were 14.1, 7.5, and 9.2 μM, respectively [17]. For CB-3, the LC and the IC_{50} were not obtainable even

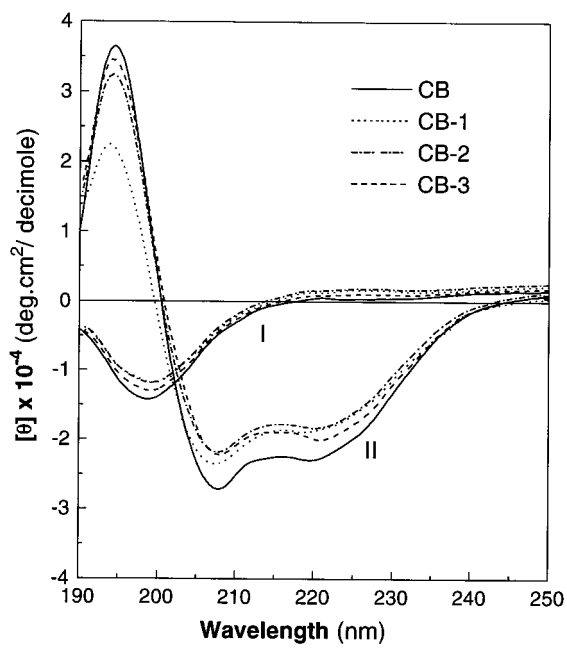

Figure 2 CD spectra of the peptides, CB, CB-1, CB-2, and CB-3 without (I) and with (II) 20% (v/v) HFP.

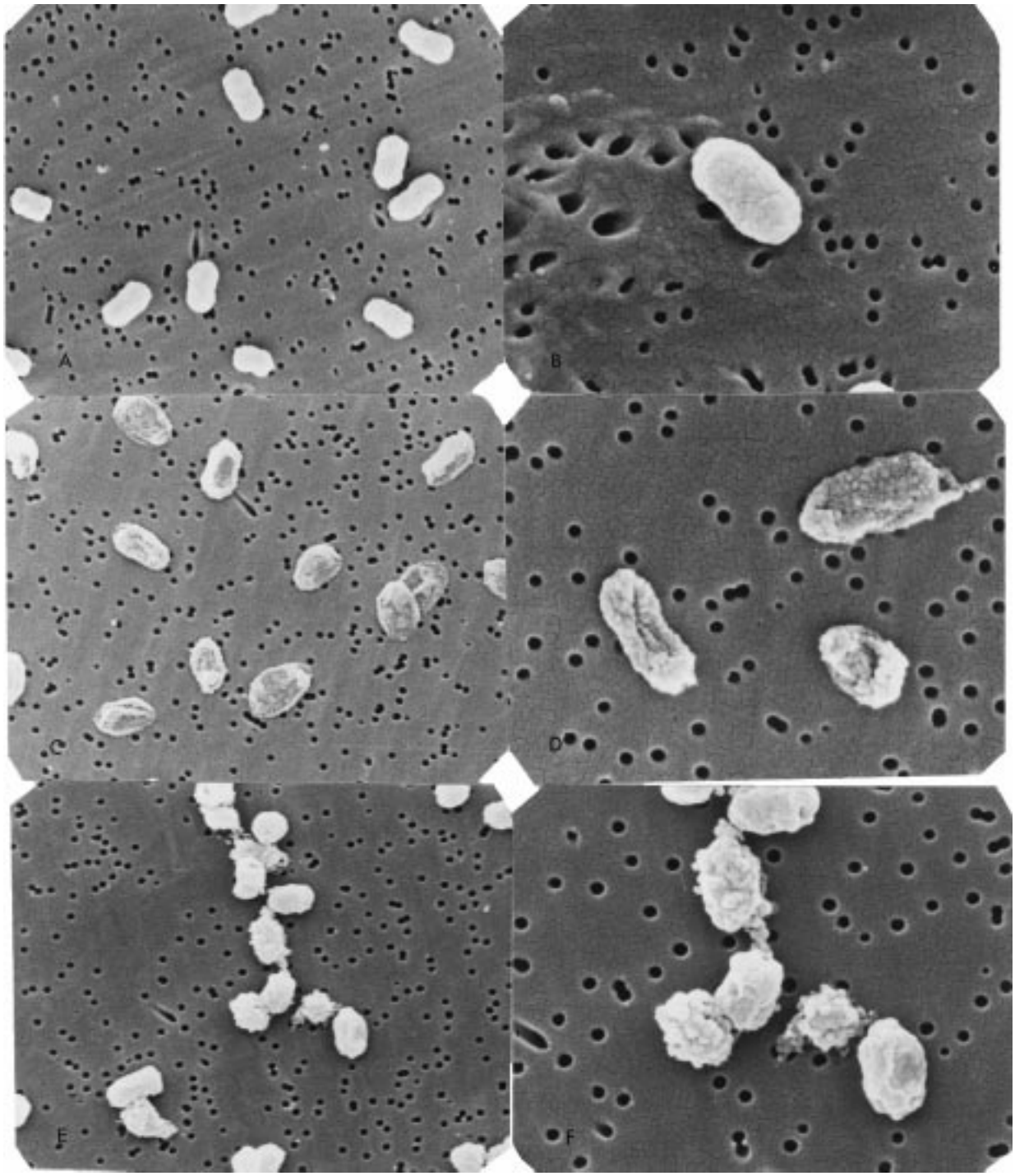

Figure 3 SEM micrographs of KP. (A) and (B) KP without peptide. (C) and (D) KP treated with CB for 2 h. (E) and (F) KP treated with CB-1 for 2 h. Magnifications are 10 K× for (A), (C) and (E) and 20 K× for (B), (D) and (F).

when the peptide concentration was increased to 50 μM. Since CB-3 has negligible effects on KP and HL-60, it was excluded from both the SEM and the TEM investigations.

SEM of the Effects of CB, CB-1 and CB-2 on KP

Typical SEM photographs of the effects of CB and CB-1 on KP are shown in Figure 3. Healthy cells (KP_{normal}) have an oval-like shape with a regular and

smooth surface (see Figure 3A and B). Damaged cells induced by CB (KP_{CB}; Figure 3C and D) and CB-1 (KP_{CB-1}; Figure 3E and F) were found to have irregular and bleb-like protrusions on their surfaces. Figure 3B, D and F are at two-fold magnification compared with Figure 3A, C and E, respectively. Based on two-dimensional measurements, we observed, in general, that the cells were swollen or shrunken after treatment with CB or CB-1, respectively. By considering the cells to be elliptical, KP_{CB} cells have the largest dimensions, while KP_{CB-1} cells possess the smallest dimensions and KP_{normal} cells are in the middle. For CB-2 treated cells, we observed similar effects to those seen for CB-1 treated cells (SEM data not shown).

TEM of the Effects of CB, CB-1 and CB-2 on KP

After the incubation of KP with cecropin B and its analogs, CB-1 and CB-2, for 2 h, TEM micrographs were taken in the major-axis section view (MASV) and the minor-axis section view (MISV) and are shown in Figure 4. MASV and MISV micrographs of KP_{normal} cells (Figure 4A and B, respectively) show normal ellipse-like shapes. After the cells were treated with cecropin and its analogs, different shapes were observed in the bacteria. KP_{CB} cells show a more convex shape (Figure 4C — MASV, D — MISV) and KP_{CB-1} cells show a more concave shape (Figure 4E — MASV, F — MISV). When compared with KP_{normal} cells, KP_{CB-2} cells showed a similar effect to KP_{CB-1} cells (TEM data not shown).

SEM of the Effects of CB, CB-1 and CB-2 on HL-60

Some typical SEM photographs of normal HL-60 cells ($HL\text{-}60_{normal}$) and cecropins (CB, CB-1 and CB-2) treated HL-60 cells ($HL\text{-}60_{CB}$, $HL\text{-}60_{CB-1}$, and $HL\text{-}60_{CB-2}$, respectively) are shown in Figure 5. The results show that the $HL\text{-}60_{normal}$ cells (Figure 5A) are rounded and covered by bulbous projections and small hair-like processes (Figure 5B). $HL\text{-}60_{CB}$ cells show bleb-like shapes (Figure 5C) and many rounded protrusions extending from the cell surface can be observed (Figure 5D). The extent of the aggregation of the dead $HL\text{-}60_{CB}$ cells (Figure 5C) is higher than that of live cells $HL\text{-}60_{normal}$ (Figure 5A). For $HL\text{-}60_{CB-1}$ and $HL\text{-}60_{CB-2}$ cells, a large number of broken shreds can be observed on the cell surfaces (Figure 5E and F, respectively). The morphological changes in the cells treated with CB-1 and CB-2 are different from those of cells treated with CB.

TEM of the Effects of CB, CB-1 and CB-2 on HL-60

The TEM micrograph of an $HL\text{-}60_{normal}$ cell is shown in Figure 6A. A rounded cell (inside ring area) covered by abundant clusters of cilia and bulbous projections (outside ring area) is observed. Section views of HL-60 cells after the treatment with CB-1 and CB-2 for 15 min are shown in Figure 6B and C, respectively. These results show that the profiles of both the cell itself and the outer area are seriously distorted. Many white bubble-like lumps located outside the cell membrane were formed. The morphological changes caused in HL-60 cells were similar whether they were treated by CB-1 or CB-2. After the same incubation times, HL-60 cells treated by CB (Figure 6D) were relatively less distorted than those treated by CB-1 and CB-2. The rounded protrusions extending from the surface of $HL\text{-}60_{CB}$ cells observed by SEM (Figure 5D) correspond to the white bubble-like lumps of the similarly treated cells observed by TEM (Figure 6D).

DISCUSSION

The potencies of the natural anti-microbial peptides, cecropins, and some cecropin analogs, constructed either by minor changes (point mutations) in their sequences or by making hybrids of cecropin and other anti-bacterial peptides, have been previously investigated [5,19,20]. Most of these studies have focused on bacterial cells whereas eukaryotic cells, including malignant cells, have rarely been studied. Since the cell killing action of the peptides on cell membranes may be improved by an understanding of the interactions between lipids and the peptides, different cell membranes including those of prokaryotic and eukaryotic cells, as well as various types of peptides have to be studied. We have previously studied the potencies of CB and its analogs CB-1 and CB-2, which possess α-helical segments with different characteristics, on bacteria, liposomes and cancer cells [17]. The roles of the amphipathic and hydrophobic helices of the peptides in killing those cells have been elucidated [17]. The C-terminal hydrophobic α-helix of the natural peptide, CB, does play a role in killing bacteria, but does not appear to be required for killing cancer cells. Having two amphipathic α-helices (CB-1 and CB-2) instead of one amphipathic and one hydrophobic α-helix (CB) is more effective for killing malignant cells, but is not as important for killing bacteria.

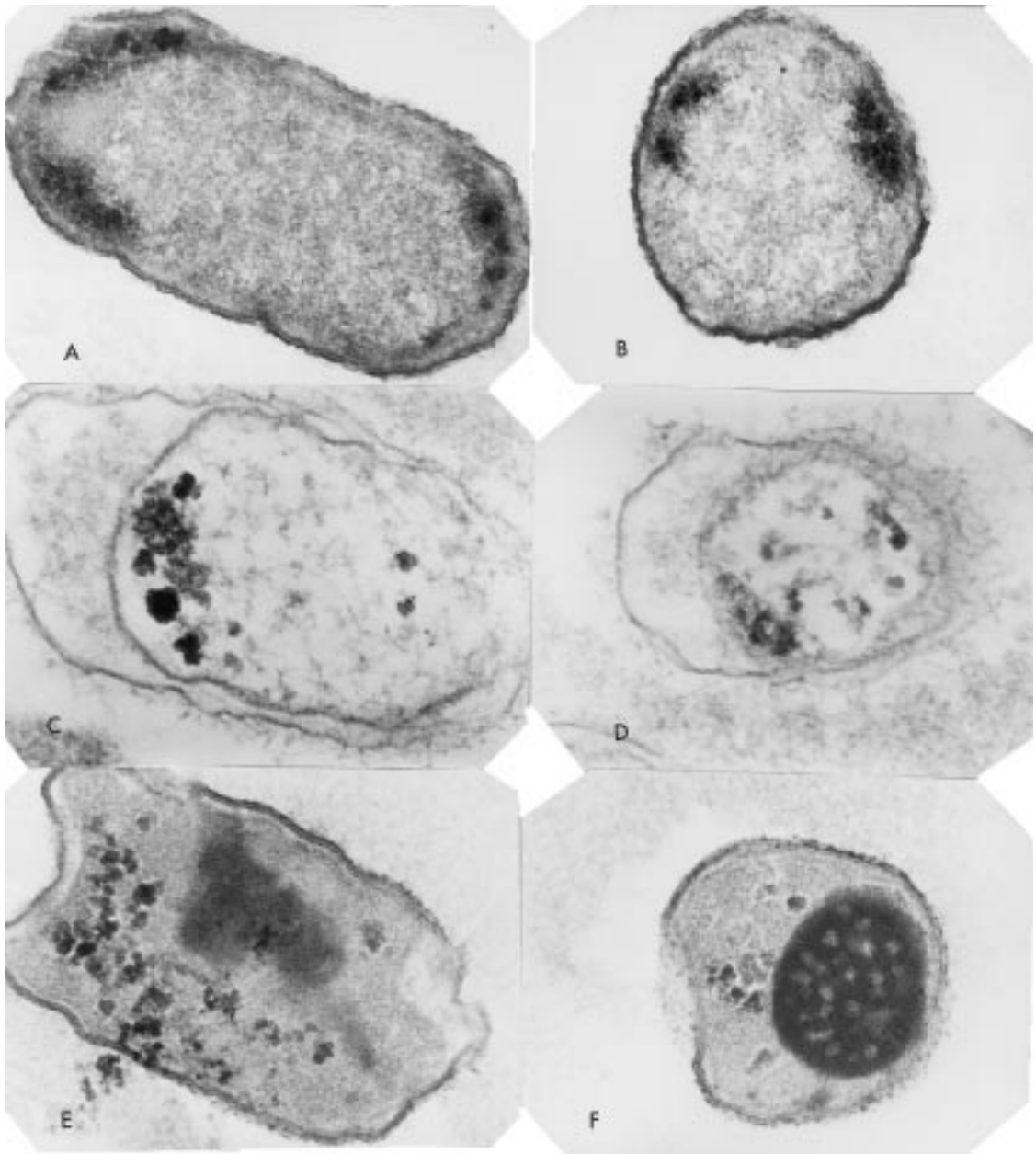

Figure 4 TEM micrographs of KP. (A), (C) and (E) MISV views and (B), (D) and (F) MISV views of KP without peptide, KP with CB and KP with CB-1, respectively.

In this paper, a related question is examined: if a peptide has two hydrophobic α-helices (CB-3) instead of one amphipathic and one hydrophobic α-helix, what is its lysing ability on both bacterial and cancer cells? The experimental results show that CB-3 has little killing effect on both bacterial and cancer cells and this indicates that hydrophobic α-helices alone are insufficient for lysing bacterial and malignant cells. However, a hydrophobic α-helix is still necessary for effective lysing of bacterial cell membranes as the potency of CB on KP is higher than that of both CB-1 and CB-2. Another possibility is that the killing potency of peptides on these cells could be due to the stability of their secondary structure, rather than the characteristics of their α-helices. In this work, the secondary structure probe, circular dichroism, has been used to investigate this question. The resultant spectra show that all peptides possess comparable secondary structures (see Figure 2) and, therefore, the

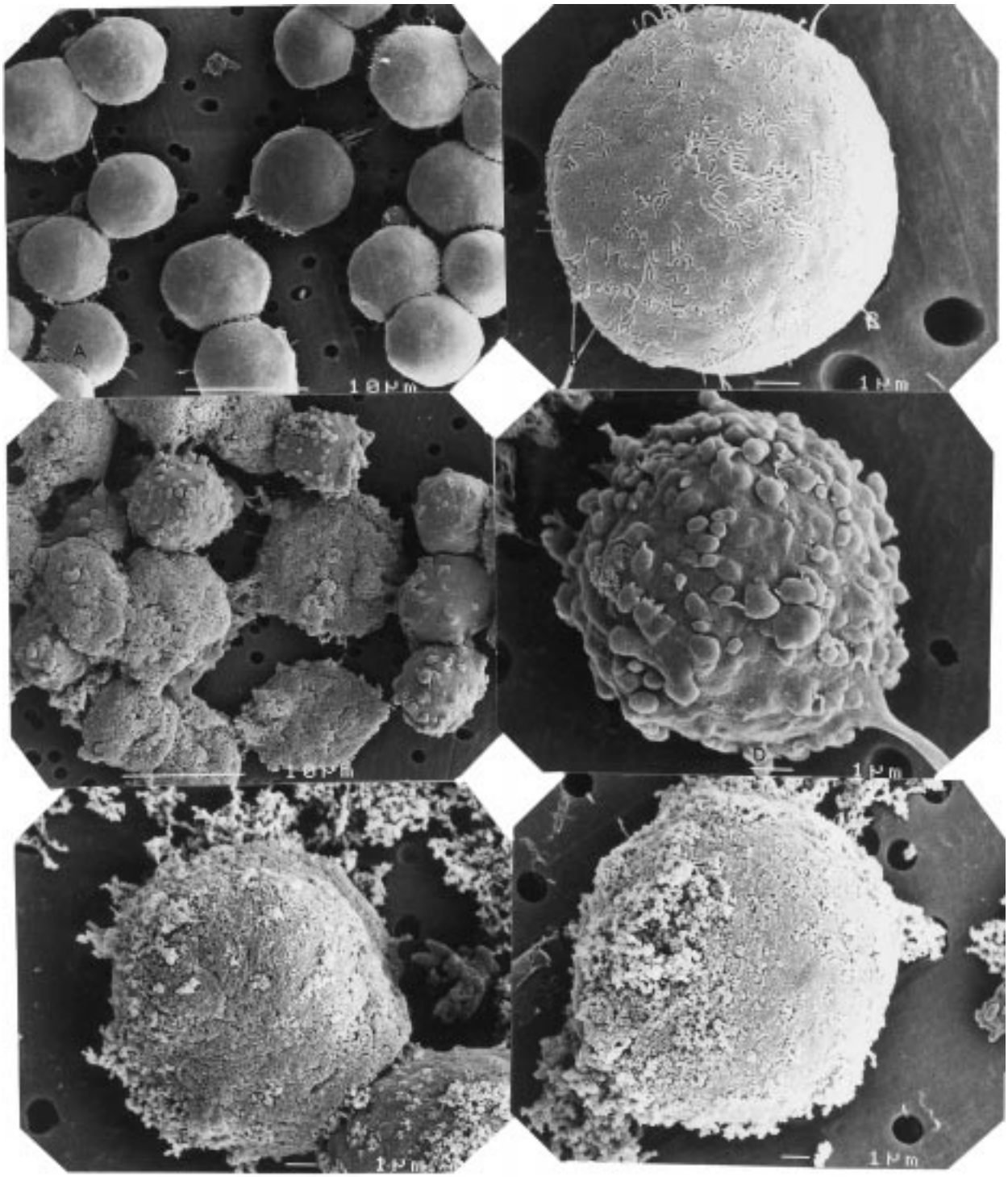

Figure 5 SEM micrographs of HL-60. (A) shows multiple cells and (B) a single cell of untreated HL-60. (C) and (D) are micrographs of multiple and single HL-60 cells treated with CB for 15 min. (E) and (F) show the morphological changes of HL-60 cells treated with CB-1 and CB-2, respectively, for 15 min. The magnification is 2.5 K × for multiple cells and 9 K × for single cells.

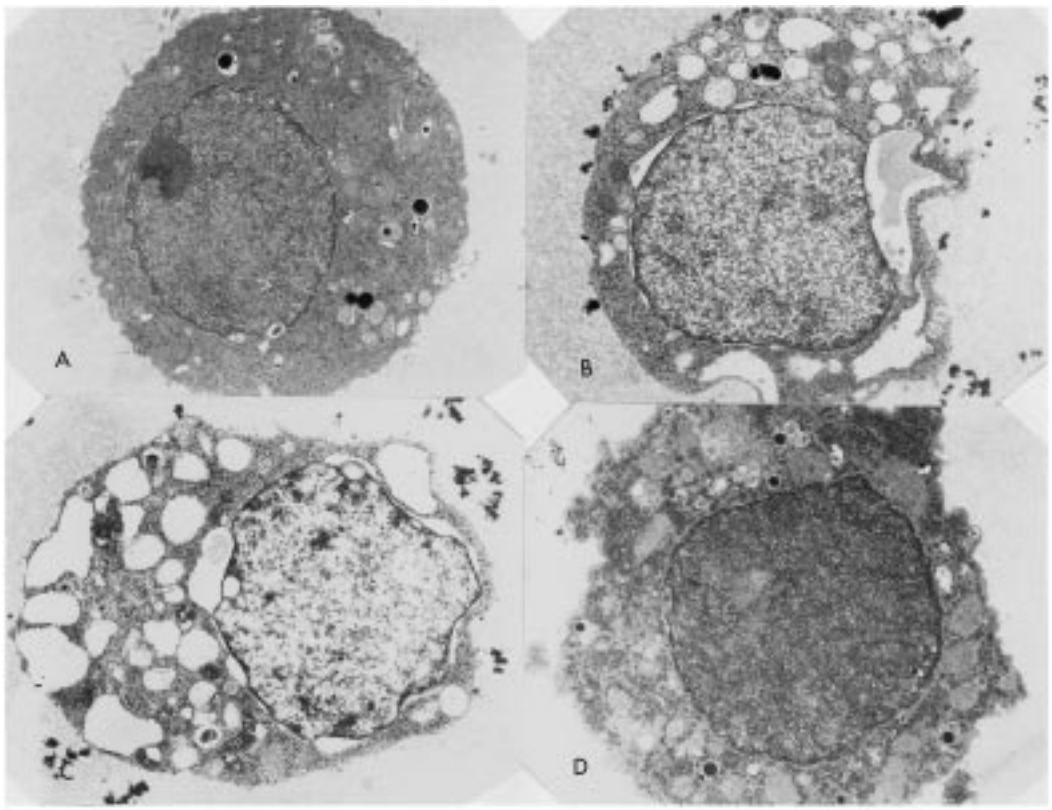

Figure 6 TEM micrographs of HL-60. (A) is an untreated HL-60 cell. (B) and (C) are HL-60 cells treated with CB-1 and CB-2, respectively, for 15 min. (D) is the HL-60 cell treated with CB for 15 min.

range of killing potencies of the different peptides results from the characteristics of their α-helices.

Based on the above observations, it is intriguing to know how cells are killed by peptides having different cell killing efficiencies? Are the killing mechanisms of the different types of peptides (such as CB, CB-1 or CB-2) the same? An understanding of the morphological changes induced in cells by these peptides is necessary before their cell killing mechanisms can be completely elucidated. Both SEM and TEM techniques have been used to gain this understanding. Figure 3 shows SEM micrographs of the morphological changes in the bacterium, KP, induced by CB and CB-1. It can be seen that the action of the peptides has caused changes in the dimensions and shape of the cells. These results were reproducible and the number of cells killed by the mechanical operations of sample preparation was small. On average, cells treated with CB (Figure 3C and D) expanded ('swelling') while those treated with CB-1 (Figure 3E and F) contracted ('shrinking') when compared with untreated cells (Figure 3A and B).

The 'swelling' and 'shrinking' phenomena induced by CB and CB-1, respectively, on KP cells were further investigated by TEM. Figure 4C and D show the swelling between the outer and inner-membranes of the cell caused by the action of CB. In general, the outer membrane has been separated from the inner membrane of the cell. The swollen area between these two membranes may be caused by the in-take of water from the medium into the cell. The cell membrane breaking (penetration) rate of CB may be retarded by CB's hydrophobic helix being retained in the hydrophobic tail area of the lipid bilayer. As water and other ions pass through the channels in the outer membrane, the separation of the two lipid bilayers will increase, probably further inhibiting the passage of CB to the inner membrane. The development of the process of cell death appears to be restricted to the region between the outer and inner cell membranes. This observation is similar to the effect of melittin on *Escherichia coli* [21]. An experiment where *Escherichia coli* was treated with synthetic CB has shown a similar effect in breaking cell membranes [22]. However, their results only showed that the formation of pores in

the cell membrane was in the final stage of cell death and the detailed morphological changes of the membrane were not observed.

For CB-1 treated cells the situation is opposite to that of CB treated cells. Figure 4E and F show the shrunken shapes of the cells after treatment with CB-1. A possible interpretation is that as CB-1 has two amphipathic helices it passes through the outer membrane without being retained in the lipid bilayer as CB appears to be. It can then pass through the inner membrane before extracellular water can enter the cell. The imbalance of osmotic forces between the inner and outer membranes causes cytoplasm to leak from the cell causing distortion and shrinkage. Therefore, the killing mechanisms of CB and CB-1 on KP cells are completely different. However, it is not immediately clear why the killing efficiency of CB is higher that that of CB-1 on KP cells. A possible explanation is that the leakage of cell cytoplasm to the outside medium is more difficult than the intake of water from the buffer into the inter membrane area. The formation of ion channels by CB [23,24] may allow water to pass through more readily than the pores formed by CB-1 or CB-2 allowing cytoplasm to pass through. Therefore, more CB-1 or CB-2 than CB may be needed to create the conditions for cell death. Another contribution to the higher efficiency of CB on bacterial cells may come from the hydrophobic helix assisting in retaining the peptide in the membrane, while the amphipathic helices of CB-1 or CB-2 may be released after an initial penetration.

The cytotoxicity of cecropin B and its analogs, CB-1 and CB-2, on cancer cells by observing their morphological changes during the development of cell death were explored. Figure 5A and B show the SEM micrographs of HL-60 cancer cells which are very different from those treated with CB (Figure 5C and D), CB-1 (Figure 5E) or CB-2 (Figure 5F). Among the treated cells, the morphological change caused by CB is different from that caused by either CB-1 or CB-2. However, the cells treated with CB-1 and CB-2 show similar changes. This indicates that the killing pathway of CB is not the same as that of CB-1 or CB-2; i.e., the replacement of a hydrophobic α-helix by an amphipathic α-helix can alter the process of cell killing. TEM micrographs of the broken cells induced by CB-1, CB-2 and CB are shown in Figure 6B, C and D, respectively. In all the cell killings induced by these peptides, the membranes become badly twisted leading to cell death. The killing efficiency of CB-1 and CB-2 on these cancer cells is higher than that of CB. A possible interpretation is that the higher cationic content (four extra cationic residues) of CB-1 and CB-2 when compared with CB leads them to have higher affinities for the tumor cell which has a greater anionic nature in its membrane [25]. These peptides may then be more effectively retained in the anionic membrane, disrupting it more efficiently than the less cationic CB. It is probable that the peptides associate differently once retained in the membrane causing the different morphological features observed.

In this paper, we used the different concentrations of the peptides to induce the lysis of KP and HL-60 cells and observed that the morphological changes were similar if the same kind of peptide was used. To optimize the observations, the cell morphological changes induced by a higher dose of the peptides (50 μM) were shown. Regardless of the doses, these results indicate that a different killing pathway leading to a particularly morphological change of the cells exists. The amount of peptides on the cells reflects only the population change of the dead cells. We believe that the different LC values of peptides on bacteria are due to their killing efficiency. The different efficiency may be a result of the different killing pathways causing different morphological changes in the cells. This prediction is especially valid for the double-membrane cells, like bacteria, when the TEM results shown in Figure 4 are examined. For the transformed cell, the morphological changes induced by different characteristics of the peptides are not clear as compared with the bacteria induced by the same peptides. The possible reason is that the abundant clusters of cilia and bulbous projections covering the cell membrane play a significant role during the killing action. The morphological changes in this area thus overlook the deformations of the membranes. However, in statistics, we observed that the morphological changes of the cancer cells induced by CB and CB-1/CB-2 were different (see Figure 5) before the cells are completely destroyed and followed by the aggregation.

CONCLUSIONS

How is the permeabilization effect of the lytic peptides on membranes achieved and how is the cell leakage induced by these peptides remain open questions [26]. Two proposed killing mechanisms, pore formation [23,27,28] and detergent effect [19,29], have been reported. However, these predictions were identified only either by models or by theories. Evidence for real observations was absent.

In this paper, we have used peptides with different characteristics to treat bacterium and cancer cells and found that their morphological changes were different. These changes are not due to dose-dependent action. For the bacterium, KP, the phenomena of 'swelling' and 'shrinking' during the cytolysis induced by CB and CB-1/CB-2, respectively, were observed. These appear to be caused by an influx of water into the cell membrane and the leakage of cytoplasm, respectively, due to the type of the pores formed by the peptides. The greater cytolytic capacity of CB on KP cells may be due to the influx of water being more efficient than the leakage of cytoplasm or to CB being more readily retained by the bacterial cells. On cancer cells the greater cytolytic capacity of the more cationic CB-1 and CB-2 may be attributable to their being retained more readily on the anionic membrane. Further development of lipid bilayer models to explain these different modes of action are proceeding.

Acknowledgements

This work was supported by grants HKUST 519/94M from the Hong Kong Research Grants Council and DAG 96/97.SC02 from the Hong Kong University of Science and Technology. We are grateful to Dr Dennis McMaster for his help with peptide synthesis.

REFERENCES

1. H. Steiner, H. Bennich, H.G. Boman, A. Engstrom and D. Hultmark (1981). Sequence and specificity of 2 anti-bacterial proteins involved in insect immunity. *Nature 292*, 246–248.
2. H.G. Boman (1991). Antibacterial peptides: key components needed in immunity. *Cell 65*, 205–207.
3. D. Hultmark (1993). Immune-reactions in *Drosophila* and other insects—a model for innate immunity. *Trends Genet. 9*, 178–183.
4. J.-Y. Lee, A. Boman, S. Chauanxin, M. Anderson, H. Jornvall, V. Mutt and H.G. Boman (1989). Antibacterial peptides from pig intestine: isolation of a mammalian cecropin. *Proc. Natl. Acad. Sci. USA 86*, 9159–9162.
5. D. Hultmark, A. Engstrom, H. Bennich, R. Kapur and H.G. Boman (1982). Insect immunity: isolation and structure of cecropin D and four minor antibacterial components from cecropia pupae. *Eur. J. Biochem. 127*, 207–217.
6. A.J. Moore, P.M. Loadman, D.A. Devine and M.C. Bibby (1995). Extraction of the synthetic lytic peptide, cecropin B, from biological fluid and analysis using reversed-phase high performance liquid chromatography. *J. Chromatgr. B 672*, 225–231.
7. R.B. Merrifield, H.G. Boman and L.D. Vizioli (1982). Synthesis of the antibacterial peptide cecropin A (1-33). *Biochemistry 21*, 5020–5031.
8. F.M. Ausubel, R. Brent, R.E. Kingston, D.D. Moore, J.G. Seidman, J.A. Smith and K. Struhl: *Current Protocols in Molecular Biology*, Green Publishing Associates and Wiley-Interscience, John Wiley and Sons, Inc., New York 1990.
9. J.E. Callaway, J. Lai, B. Haselbeck, M. Baltaian, S.P. Bonnesen, J. Weickmann, G. Wilcox and S.-P. Lei (1993). Modification of the C terminus of cecropin is essential for broad-spectrum antimicrobial activity. *Antimicrob. Agents Chemother. 37*, 1614–1619.
10. V. Lorian: *Antibiotics in Laboratory Medicine*, 4th edition, Williams and Wilkins, Baltimore 1996.
11. H.G. Boman (1995). Peptide antibiotics and their role in innate immunity. *Annu. Rev. Immunol. 13*, 61–92.
12. C.E. Dempsy (1990). The actions of melittin on membranes. *Biochim. Biophys. Acta 1031*, 143–161.
13. M.S.P. Sansom (1991). The biophysics of peptide models of ion channels. *Prog. Biophys. Mol. Biol. 55*, 139–235.
14. M. Zasloff (1987). Magainins, a class of antimicrobial peptides from *Xenopus* skin—isolation, characterization of 2 active forms, and partial cDNA sequence of a precursor. *Proc. Natl. Acad. Sci. USA 84*, 5449–5453.
15. T. Ganz, M.E. Selsted and R.I. Lehrer (1990). Defensins. *Eur. J. Hematol. 44*, 1–8.
16. A.J. Moore, D.A. Devine and M.C. Bibby (1994). Preliminary experimental anticancer activity of cecropins. *Peptide Res. 7*, 65–269.
17. H.M. Chen, W. Wang, D. Smith and S.C. Chan (1997). Effects of the anti-bacterial peptide cecropin B and its analogs cecropin B-1 and B-2, on liposomes, bacteria and cancer cells. *Biochim. Biophys. Acta 1336*, 171–179.
18. W.O. Foye: *Cancer Chemotherapeutic Agents*, ACS Professional Reference Book, American Chemical Society, Washington, DC 1995.
19. D.D. Ourth, T.D. Lockey and H.E. Renis (1994). Induction of cecropin-like and attacin-like antibacterial but not antiviral activity in heliothis virescens larvae. *Biochem. Biophys. Res. Commun. 200*, 35–44.
20. H.G. Boman, D. Wade, I.A. Boman, B. Wahlin and R.B. Merrifield (1989). Antibacterial and antimalarial properties of peptides that are cecropin-melittin hybrids. *FEBS Lett. 259*, 103–106.
21. W.G. Henk, W.J. Todd, F.M. Enright and P.S. Mitchell (1995). The morphological effects of two antimicrobial peptides, hecate-1 and melittin, on *Escherichia coli*. *Scanning Microsc. 9*, 510–507.

22. T.D. Lockey and D.D. Ourth (1996). Formation of pores in *Escherichia cold* cell membranes by a cecropin isolated from hemolymph of heliothis virescens larvae. *Eur. J. Biochem. 236*, 263–271.
23. B. Christensen, J. Fink, R.B. Merrifield and D. Mauzerall (1988). Channel-forming properties of cecropins and related model compounds incorporated into planar lipid membranes. *Proc. Natl. Acad. Sci. USA 85*, 5072–5076.
24. M. Oblatt-Montal, M. Yamazaki, R. Nelson and M. Montal (1995). Formation of ion channels in lipid bilayers by a peptide with the predicted transmembrane sequence of botulinum neurotoxin A. *Protein Sci. 4*, 1490–1497.
25. W.J. Van Blitterswijk, G. De Veer, J.H. Krol and P. Emmelot (1982). Comparative lipid analysis of purified plasma membranes and shed extracellular membrane vesicles from normal murine thymocytes and leukemic GRSL cells. *Biochim. Biophys. Acta 688*, 495–504.
26. J.M. Mancheno, M. Onaderra, A.M. Delpozo, P. Diaz-Achirica and D. Andreu (1996). Release of lipid vesicle contents by an antibacterial cecropin A-melittin hybrid peptide. *Biochemistry 35*, 9892–9899.
27. A.V. Gomes, A. Dewaal, J.A. Berden and H.V. Westerhoff (1993). Electric potentiation, cooperativity and synergism of magainin peptide in protein-free liposomes. *Biochemistry 32*, 5356–5372.
28. L. Silvestro, K. Gupta, J.N. Weiser and P.H. Axelsen (1993). The concentration-dependent membrane activity of cecropin A. *Biochemistry 36*, 11452–11460.
29. Y. Pouny, D. Rapaport, A. Mor, P. Nicolas and Y. Shai (1992). Interaction of antimicrobial dermaseptin and its fluorescently labeled analogs with phospholipid-membranes. *Biochemistry 31*, 12416–12423.

